Published in final edited form as:
Biomacromolecules. 2017 May 08; 18(5): 1449–1459. doi:10.1021/acs.biomac.7b00068.

Enhancing Tumor Penetration of Nanomedicines

Qingxue Sun[a], **Tarun Ojha**[a,b], **Fabian Kiessling**[a], **Twan Lammers**[a,b,c], and **Yang Shi**[a,*]

[a]Department of Nanomedicine and Theranostics, Institute for Experimental Molecular Imaging, RWTH Aachen University Clinic, 52074 Aachen, Germany [b]Department of Pharmaceutics, Utrecht Institute for Pharmaceutical Sciences, Utrecht University, Utrecht, 3584 CG, The Netherlands [c]Department of Targeted Therapeutics, MIRA Institute for Biomedical Technology and Technical Medicine, University of Twente, Enschede, 7522 NB, The Netherlands

Abstract

Tumor-targeted nanomedicines have been extensively applied to alter the drawbacks and enhance the efficacy of chemotherapeutics. Despite the large number of preclinical nanomedicine studies showing initial success, their therapeutic benefit in the clinic has been rather modest, which is partially due to the inefficient tumor penetration caused by tumor microenvironment (high density of cells and extracellular matrix, increased interstitial fluid pressure). Furthermore, tumor penetration of nanomedicines is significantly influenced by physicochemical characteristics such as size, surface chemistry and shape. The effect of size on tumor penetration has been exploited to design nanomedicines with switchable size to tackle this challenge. Moreover, several pharmacological and physical approaches have been developed to enhance the tumor penetration of nanomedicines, by penetration-promoting ligands, intratumoral drug release, and modulating the tumor microenvironment and vasculature. Overall, these efforts have resulted in nanomedicines with better tumor penetration properties and with enhanced therapeutic efficacy. Future research should be directed to penetration-promoting strategies with broad applicability and with high translational potential.

Keywords

nanomedicine; tumor penetration; extravasation; microenvironment; stimuli-sensitive

Introduction

Chemotherapy serves as one of the most important cancer treatment modalities. Despite of the extensive clinical usage, conventional chemotherapeutic drugs encounter several disadvantages. Due to their low molecular weight, they in general have low half-lives in the blood and are non-ideally and rapidly distributed in healthy tissues and organs, which limit the therapeutic efficacy and induce serious side effects. Several decades ago, nanoparticles (NPs) including liposomes, polymeric micelles, polymer-drug conjugates have been utilized

*Corresponding author: Department of Nanomedicines and Theranostics, Institute for Experimental Molecular Imaging (ExMI), RWTH Aachen University Clinic, 2074 Aachen, Germany, yshi@ukaachen.de (Y. Shi).

Europe PMC Funders Author Manuscripts

for tumor-targeted delivery of chemotherapeutic drugs (termed as nanomedicines), which is realized via passive targeting (Enhanced Permeability and Retention (EPR) effect) and/or active targeting (surface functionalization of NPs with targeting ligands) mechanisms.1–4

However, although nanomedicines have often shown greatly enhanced therapeutic efficacy in preclinical studies compared to conventional chemotherapeutic drugs, their efficacy in clinical setting is suboptimal due to the heterogeneity of the EPR effect,5 and the biological barriers of tumors hindering effective penetration of NPs.6–8 Tumor tissues are characterized by a high density of extracellular matrix (ECM) and cells, and leaky vasculature and impaired lymphatic circulation which overall result in a high interstitial fluid pressure (IFP).9 These factors together form a biological barrier that prevents nanomedicines from penetrating into tumor tissues, as it is frequently observed that nanomedicines mainly locate around blood vessel walls of tumors and hardly diffuse deeper into tissues.10 Recently Kataoka and colleagues reported that the extravasation and permeation of NPs through tumor blood vessels occurs in a dynamic manner characterized by vascular bursts followed by brief vigorous outward flow of fluid (eruptions).11

Tumor penetration of nanomedicines is highly dependent on their physicochemical characteristics (size, surface charge and particle shape), and tuning these factors has shown to enhance tumor penetration. For instance, polymeric micelles (PM) with smaller size better penetrate into tumor interstitium.12 However, excessive tuning of the physicochemical characteristics of nanomedicines can compromise their targeting efficiency, e.g., minimizing particle size below 5 nm shortens their blood circulation and therefore tumor targeting efficiency. To tackle this dilemma, researchers have developed nanomedicines with switchable size triggered by endogenous stimuli (e.g., low pH, high concentration of matrix metalloproteinases (MMPs)) and external stimuli (e.g., light). These nanomedicines have suitable physicochemical properties that ensure prolonged blood circulation and targeting efficiency, and decreased particles that have enhanced tumor penetration capability.

Other nanomedicine approaches to enhance tumor penetration have been realized by penetration-promoting ligands, which mostly involves NPs surface conjugation with penetration-promoting ligands, and by intratumoral release that results in liberation of small molecules with better diffusion in tumor interstitium. Moreover, as described above, the pathological properties of tumors result in compromised penetration of nanomedicines, and therefore strategies to reverse or to modulate the tumor microenvironment via pharmacological and physical resorts have been applied to enhance tumor penetration. Finally, various methods to evaluate penetration of nanomedicines using in vitro and in vivo models have been developed.

This review summarizes the physicochemical properties of nanomedicines that influence their penetration in tumor tissues, and discusses nanomedicine approaches and physical/pharmacological strategies to modulate the tumor microenvironment for enhancing their penetration. Overall, research in this regard has the potential to forward nanomedicines to the next level that ensures robust clinical benefit.

1 Physicochemical characteristics of nanomedicines affecting tumor penetration

1.1 Particle size

Particle size of nanomedicines is one of the most important characteristics influencing their in vivo fate, including blood circulation kinetics, biodistribution and localization in target tissues. Results from different groups have shown that in general smaller particles size corresponds to better tumor penetration. Pioneering research performed by Dreher, Chilkoti and colleagues studied the tumor penetration of dextrans with molecular weights ranging from 3.3 kDa to 2 MDa corresponding to sizes from 3.5 to 50 nm. In vivo results showed that the penetration depths of both 3.3 and 10 KDa dextrans were more than 35 μm 30 min after intravenous (i.v.) injection, two times higher than those of 40 and 70 KDa (15 μm). Dextran of 2 MDa only penetrated for 5 μm into the tumor tissues in the same time frame.13 Jain, Bawendi and colleagues showed that the tumor penetration of quantum dots (QDs) with decreasing size from 125 to 12 nm was increased from 40 to 80 μm in Mu89 tumors in SCID mice.14 A similar relationship between particle size and tumor penetration was also observed by Kataoka and colleagues for drug-loaded PM, especially for poorly perfused tumors. 1,2-diaminocyclohexane-platinum(II) (DACHPt)-loaded PM with size ranging from 30 to 100 nm were fabricated by changing the ratio between the homopolymer P(Glu) and the block copolymer PEG-b-P(Glu). Their results showed that the average tumor accumulation of all PM formulations were around 10% IDg^{-1} tumor at 24 h post-injection. PM smaller than 50 nm could effectively penetrate into the interstitium of poorly permeable pancreatic tumor in vivo, whereas the larger ones mostly accumulated at the periphery of tumors.12 The same correlation between particles size and tumor penetration was observed for PM,15 folate modified PEG-rhodamine NPs16 and ultrasmall gold NPs (AuNPs).17 All results above exclusively point to that better tumor penetration can be achieved by smaller NPs, based on a variety of materials and structures, indicating the robustness of this correlation.

1.2 Surface chemistry

Surface charge is another influential physicochemical characteristic of nanomedicines for their penetration in tumors. However, current research from different groups shows contradictory results regarding the effect of surface charge on tumor penetration. For example, liposomes with anionic surface charge showed better penetration than those with cationic surface charge.18, 19 A similar phenomenon has been observed for gold nanorods (AuNRs) with the size of 55×14 nm (length×dimameter), i.e., the negative ones were more effective regarding penetration compared to the positive or neutral counterparts in a multicellular tumor spheroid model in vitro.20 However, in another study using PLGA NPs of around 165 nm, it was reported that slightly positive NPs (+4 mV) achieved better tumor penetration than the negative ones (-13 mV) in mice bearing MDA-MB-231 xenografts.21 In another study, cationic lipidic NPs of around 100 nm showed increased penetration in three-dimensional (3D) tumor spheroids than anionic and neutral NPs of comparable size.22 Overall, the relationship between surface charge and tumor penetration of NPs has not been clearly elaborated, which can be simultaneously dependent on the tumor pathological

properties and other characterizations of NPs. Further studies in this regard are required to define the effect of surface charge on tumor penetration of nanomedicines.

Surface PEGylation is known for its effective improvement in blood circulation kinetics of nanomedicines,23 furthermore, dense surface PEGylation was reported to enhance penetration of NPs in malignant glioma following intracranially administration. Due to the hydrophilic and uncharged nature of PEG, PEGylation minimized interactions between PLGA NPs and charged or hydrophobic components of ECM, and therefore resulted in enhanced penetration of the NPs in rat gliomas as reported by Hanes and colleagues. Paclitaxel (PTX)-loaded PLGA NPs with dense PEG modification showed 100-fold faster penetration than similarly sized PTX-loaded PLGA NPs without PEG coatings in vivo, and significantly improved tumor suppression than non-PEGylated counterpart.24 Therefore, surface PEGylation of NPs improves their tumor penetration by minimizing interactions between NPs and tumor ECM.

1.3 Particle shape

Apart from the size and surface chemistry of NPs, shape plays an important role in tumor penetration. For example, tumor penetration of filamentous viral NPs was deeper than that of spherical ones in ovarian tumor xenografts.25 Jain and colleagues showed that penetration of nanorods (NRs) in orthotopic E0771 mammary tumors was 1.7 times the volume to that of nanospheres with the same hydrodynamic diameter (33–35 nm) at 1 h post-injection in mice. 26 Gambhir and co-workers compared the tumor penetration of spherical QDs and single-walled carbon nanotubes in three mouse tumor models (SKOV-3, U87MG and LS174T). Their results showed that the two types of NPs exhibited different tumor penetration only in the latter two models. In LS174T tumors, the QDs performed better than single-walled carbon nanotubes, whereas in U87MG, a reversed result was observed.27 AuNPs in the forms of NRs, nanocages, nanospheres and nanodisks were intravenously injected in mice bearing EMT6 breast tumor, and results showed that NRs and nanocages penetrated into the cores of the tumors, whereas nanospheres and nanodisks were retained at the rim of the tumors.28 For rod-shaped NPs, the aspect ratio affects their tumor penetration depth. Rod-shaped NPs based on tobacco mosaic virus with aspect ratios (AR) of 3.5, 7 and 16.5 (PEGylated or RGD-targeted) were intravenously injected in mice bearing HT-29 tumor xenografts, and the PEGylated NRs with AR of 3.5 had the highest tumor accumulation, whereas for RGD modified NPs, NPs with AR 7 were the most effective for tumor penetration.29 Overall, although dependent on tumor type, NPs in the round shape are associated with lower tumor penetration capability than NPs in other shapes in most of studies above, which should be taken into consideration in the design of clinical nanomedicines.

2 Approaches to enhance tumor penetration of nanomedicines

2.1 Size switchable nanomedicines

NPs < ~250 nm are prone to extravasation through the leaky tumor vasculature and consequently accumulation in solid tumors. However, due to the tumor microenvironment, penetration of large NPs is hampered, which causes ineffective killing of cancer cells distant

from tumor vessels. As discussed above in Section 1.1, down tailoring the size of NPs enhances their penetration in tumor tissues.7 However, NPs with size < 5 nm are rapidly cleared by renal filtration, which causes ineffective tumor targeting.9 Such dilemma can be subtly tackled by size tuning NPs which have size above 5 nm ensuring the prolonged blood circulation to exploit the EPR effect, and have decreased size at the tumor site to promote extravasation. To trigger the size tuning of NPs, endogenous stimuli (low pH, overexpressed MMPs) and external stimulus (light) have been applied.

2.1.1 Low pH—The pH value of tumor microenvironment (~6.5-7.0) is lower than that of normal tissues and blood (~7.4), which can be exploited to trigger degradation of acid-cleavable linkers or polarity change of ionizable chemical groups. Wang and colleagues have shown that by designing self-assembled NPs with an acid-cleavable linker, size tuning of NPs can be achieved inside tumor tissues. Polymeric clustered NPs (iCluster) were prepared with platinum prodrug-conjugated poly(amidoamine)-graft-polycaprolactone, polycaprolactone (PCL) and PEG-b-PCL (PCL-CDM-PAMAM/Pt, depicted in Figure 1 A&B). In iCluster, PAMAM/Pt was linked to the particle core via a pH sensitive degradable linker, which was cleaved in the acidic tumor extracellular environment as shown in tumor spheroids (Figure 1 C and D). After entering tumor tissues with lower pHs following i.v. injection, PAMAM/Pt of ~5 nm was released from the iCluster (~100 nm) and showed significantly improved tumor penetration than larger NPs (Figure 1 E and F).30 A similar approach has been developed by the same group using amphiphilic polymer containing tertiary amine groups that rapidly respond to pH changes. The polymer self-assembled into NPs at a relatively high pH, which were disintegrated at mild acidic pH (~6.5-7.0) due to the ionization of tertiary amine groups present in the polymer, and this process triggered size tuning of the NPs. Their in vivo results showed that, after the pH-responsive NPs (~80 nm) accumulated in tumor tissue following i.v. injection, smaller NPs of sub-10 nm were generated, which showed significantly improved tumor penetration compared to pH-insensitive NPs with a constant size of around 80 nm.31

The size down-tuning strategy has also been applied to enhance tumor penetration of inorganic NPs. Liu and colleagues synthesized MnO_2 NPs coated with human serum albumin (HSA), which were loaded with chlorine e6 and a prodrug of cis-platinum. They hypothesized that MnO_2 rapidly reacts with H_2O_2 to produce O_2 and is decomposed under acidic pH, leading to disassembly of HSA coated MnO_2 NPs. The hypothesis was validated in multicellular tumor spheroids under pH 6.8 in the presence of H_2O_2, in which chlorine e6 was significantly more widely distributed in the spheroids.32 Another approach to realize size tuning of inorganic NPs was developed by modifying small AuNPS (~13 nm) with i-motif binding oligodeoxynucleotides (ODNs) and bcl-2 antisense ODN. Clustered AuNPs of around 150 nm were self-assembled using the i-motif sequence containing a high amount of cytosine (C) as a crosslinker, which forms a unique tetrameric structure in acidic pH due to partial hybridization of C and protonated C. Results showed that, in acidic environment, partial hybridization between the i-motif occurred and the clustered AuNPs disassembled into smaller single NPs.33 However, it has not been tested in vitro or in vivo wether the size tuning behavior of the culstered AuNPs can enhance their penetration capability.

Studies discussed above indicate that decreasing size of NPs efficiently facilitates deep tumor penetration, which has been reproduced by various groups with different NP constructions. However, a different approach based on nanogels with reversibly switchable size has also shown to enhance tumor penetration. Zhang and colleagues prepared nanogels composed of *N*-lysinal-N'-succinyl chitosan with protonatable side groups and poly(*N*-isopropylacrylamide) with a bovine serum albumin (BSA) shell. At acidic pH (4.5) in late endosomes or lysosomes, the nanogels were protonated and the surface charge was changed from -20 mV to +35 mV, leading to size increase from 200 nm to 2 μm, which caused burst of the endosomes or lysosomes. Afterwards, the nanogel shrinked to around 240 nm at pH 6.8 and migrated into other cancer cells and the repeated progress increased tumor penetration of the nanogels. Their result showed that the depth of nanogel penetration into tumors was 8 to 40 times higher than that of non-sensitive nanogels in Heps tumor bearing mice.34

Overall, pH triggered size switching of nanomedicines enhances tumor penetration in different tumor models with defferent nanocarrier constructions, even though, intra-individual difference regarding tumor pathological properties (e.g., intratumoral pH value) should not be ignored, which may play an important role in the efficacy of this approach, and should be taken into consideration in future research dealing with pH-triggered size tuning nanomedicines.

2.1.2 Overexpression of MMPs—Overexpression of MMPs occurs in various tumors, which has been employed to trigger size tuning of nanomedicines to enhance tumor penetration.35, 36 Gelatin is known to be highly degradable by MMP-2 and has been utilized to prepare size tunable NPs. For example, PEGylated gelatin NPs (100 nm) were coated with QDs (10 nm) on the surface. In an in vitro study, addition of MMP-2 to the gelatin NPs applied in collagen gel triggered migration of the QDs. The QDs coated gelatin NPs were locally injected in mice bearing HT-1080 tumor, and significant intratumoral distribution of the QDs was presented 3 h post-injection.37 A similar construction has been utilized to prepare AuNPs coated gelatin NPs, with which a size decrease from ~187 to ~59 nm was observed in the presence of MMP-2.38 Gelatin was also used to prepare NPs that were conjugated with dendrigraft poly-lysine and anchored with angiopep-2 targeting the low density lipoprotein-receptor related protein. MMP-2 mediated gelatin degradation decreased the particle size from ~186 to ~56 nm. An in vitro study in 4T1 cell spheroids showed significantly more distribution of the smaller NPs at distances of 100 and 130 μm from the edge.39

MMP-2 has been repeatedly utilized to realize size tuning of NPs, which demonstrates the robustness of this approach. However, the over-expression of MMPs might be highly heterogeneous in different tumors and patients, which is a considerable burden for further pre-clinical development of this approach. Therefore, characterization of MMPs over-expression in tumors would further strengthen the applicability of this approach.

2.1.3 Light—Light-responsive materials have been utilized to prepare size tuning nanomedicines to achieve better tumor penetration. Kohane and colleagues reported UV-induced size switchable NPs, which were based on lipids and spiropyran (SP, a family of

photochromic molecules) that undergo photoisomerization under UV illumination at 365 nm. The hydrophobic SP-C9 was converted to amphiphilic merocyanine (MC)-C9 under UV light and the size of the SP-C9 NPs was decreased via the solubility change of SP-C9 (Figure 2). Furthermore, the drug release from SP-C9 NPs was also triggered by UV illumination. ICG-loaded SP NP penetrated 8.3 ± 0.10 mm in collagen gel matrix without UV triggering, which was increased to 12.1 ± 0.02 and 16.8 ± 0.10 mm with 10 and 20 s of UV irradation.40 In a cornea model, enhanced penetration of Cy5/SP NP_H was also observed in the presence of UV. In a follow up study, they evaluated the in vivo penetration and therapeutic efficacy of the photoswitchable NPs loaded with docetaxel (DTX). DTX-loaded NPs were i.v. injected in mice bearing s.c. HT-1080 tumors, the in vivo penetration in tumor tissues was improved by UV illumination at 365 nm, which led to better therapeutic efficacy than that obtained by treatment with free drug and drug-loaded NPs without UV irradiation.41

Another type of photoswitchable NPs were prepared using polyelectrolytes (poly(diallyldimethylammonium chloride or quarternized poly(4-vinylpyridine)) and an ionic photo-isomerizable azo dye (Acid Yellow 38). After UV irradiation, the ionic photoresponsive dye was isomerized, consequently the particle size was decreased from 94 nm to 62 nm.42

It is important to note that in the above-mentioned light-triggered systems, UV was used to tune sizes of the NPs, which has intrinsic limitations including poor tissue penetration and damage to healthy tissues. In this regard, near infrared (NIR) light with higher tissue penetration depth and safety should be considered due to its improved tissue penetration and higher safety as compared to UV illumination. Moreover, light triggering in general suffers from the drawback that the effect is highly localized, therefore in case of tumor metastasis the applicability of this approach is rather limited.

2.2 Penetration-promoting ligands

Conventional active targeting ligands can compromise tumor penetration of NPs, which is described as the “binding site barrier” effect.4, 43, 44 A similar observation has been reported with antibodies two decades ago.45 However, the tumor-targeting RGD family peptides have shown to enhance tumor penetration of NPs. For example, PEG-PCL NPs were modified with two peptides, RGD and interleukin-13 peptide targeting neovasculature and glioblastoma multiforme cells, respectively. The results showed that the penetration of the dual targeting NPs was approximately 40-fold higher than that of non-modified NPs and was significantly higher than that of interleukin-13 modified NPs in C6 cell spheroids.46 Ruoslahti and colleagues screened a tumor-homing peptide—iRGD (CRGDK/RGPD/EC)—which displayed superior tumor penetration enhancing capability compared to RGD for both a small molecule compound and a nanomedicine (Abraxane) by covalent conjugation. The mechanism relies on a three-step process: the RGD motif of iRGD mediates binding to αv integrins on the surface of tumor endothelium, and thereafter a proteolytic cleavage exposes a binding motif for neuropilin-1, which mediates penetration into tissues and cells (Figure 3A).47 Interestingly, shown by the same group, co-administered iRGD without chemical conjugation also enhanced tumor penetration of small molecules and NPs to the same extent

of iRGD conjugates.48 In another study, iRGD was modified with alanine-alanine-asparagine to prepare a “tadpole”-like nRGD that retains tumor penetration effect of iRGD while target tumor associated macrophages. The nRGD modified liposomes loaded with DOX at 5 mg/kg showed increased therapeutic efficacy compared to both standard PEGylated liposomal DOX and that physically mixed with nRGD.49

There are several other ligands studied for enhancing tumor penetration of nanomedicines. Lactoferrin was conjugated to lipid-graphene nanosponges of 40 or 270 nm, the smaller nanosponges without lactoferrin conjugation showed significant higher tumor distribution than the larger ones (either bare or lactoferrin coated) in 3D tumor spheroids, and the penetration enhancement was further improved by lactoferrin conjugation via transcytosis. However, the penetration enhancement mediated by lactoferrin was less significant compared to that by smaller size.50 Neovascular endothelium targeted NPs with enhanced penetration were prepared with glycoaminoglycan (dermatan sulfate (DS) 435) that has high tumor uptake. The proposed mechanism of this approach involves shuttling of DS agents across the neovascular endothelium, following DS’s initial binding to HC-II and the other heparin-binding surface receptors. DOX-loaded NPs were intravenously injected and achieved deeper tumor tissue penetration compared to free DOX (>75 versus <25 μm), and therefore better therapeutic efficacy in MX-1 human breast xenografts.51

One obvious advantage of the ligand enabled approach is that most of the ligands, apart from promoting tumor penetration, also increases tumoral cell uptake of NPs, which is essential for NPs delivering biotherapeutics such as SiRNA and proteins. Although such effect was not intended in the examples above, it can broaden the application of penetration-promoting ligands.

2.3 Intratumoral drug release

Due to the much smaller size of low molecular weight drugs than macromolecules or nanomedicines, they have the potential to reach deep tumor tissues. One of the most known examples is based on DOX-loaded thermosensitive liposomes (DOX-TSL), which were composed of dipalmitoylphosphatidylcholine, 1-stearoyl-2-hydroxy-sn-glycero-3-phosphocholine, as well as a PEGylated lipid, i.e, 1,2-distearoyl-sn-glycero-3-phosphoethanolamine-N-PEG2000. When DOX-TSL accumulated into the preheated tumor tissues, DOX was released from the liposomes in tumor tissues and effectively penetrated in tumor interstitium. The authors showed that the penetration distance of DOX released from DOX-TSL combined with heating treatment was doubled than that of traditional liposomal DOX with preheating the tumors (78±18 μm versus 34±9 μm).52

Intratumoral drug release can also be achieved by ultrasound-induced microbubble (MB) destruction.53, 54 Klibanov and colleagues prepared lipidic MBs functionalized with calcein/thrombin-loaded liposomes via the biotin-streptavidin interaction. Application of 1 MHz ultrasound led to ~30% of calcein release in vitro as evaluated by the fluorescence quenching assay.55 In another study, lipidic MB loaded with liposomal DOX were prepared by mixing DOX-loaded liposomes with a lipid solution and subsequent high-speed shaking of the mixture. A significant DOX release from the liposomes was measured upon

ultrasound treatment, which induced increased cytotoxicity of the formulation in BLM cells compared to the same formulation without applying ultrasound.56

Apart from physical triggers, stimuli-sensitive chemistry has been applied to prepare nanomedicines with intratumoral drug release. DOX was conjugated to the aldehyde dextran NPs with an acid cleavable imine bond (Schiff base) which is rapidly hydrolyzed in the acidic environment. After localization of the NPs in tumor tissues, DOX was released due to the low pH of tumors. The tumor penetration distance of DOX conjugated in the NPs was approximate 10 times higher than that free DOX (~400-500 versus 50 μm).57

These nanoformulations with physically triggered intratumoral release have shown their improved penetration capability using different tumor models and nanocarriers, which can be ascribed to a certain extent by the robustness of externally applied triggers that are independent on pathological properties of tumors. On the other hand, the drawback of this approach is that the physical triggers can only be applied rather locally, which means that their applicability in metastasized lesions is severally compromised.

2.4 Pharmacological modulation of tumor microenvironment and vasculature

2.4.1 Degradation of ECM—Tumor ECM is composed of collagen, fibronectin, HA and proteoglycans.9, 58 It was shown that the increased fibrosis hindered the penetration of macromolecules in tumors,59 and therapeutic agents that decreases ECM could enhance tumor penetration of nanotherapeutics.60 Jain and colleagues pioneered the application of losartan, an angiotensin II receptor antagonist used in the clinic for hypertension, for enhancing tumor penetration and therapeutic efficacy of nanotherapeutics. Apart from its antihypertensive effect, losartan is also an antifibrotic agent and reduces collagen I levels in various tumor models. When injected intratumorally in losartan pre-treated HSTS26T and Mu89 mice models, polystyrene NPs of 100 nm were significantly extravasated from vessels compared to those administered in control mice without losartan pre-treatment. The enhanced tumor penetration of the NPs was achieved by losartan-induced collagen fiber disruption, as confirmed by histological examination of the tumor tissues.60 The penetration-enhancing effect of losartan has been confirmed in a study using liposomes as the drug carrier. Losartan pre-treatment of 4T1-bearing mice at 40 mg/kg was applied prior to i.v. injection of PEGylated liposomes around 100 nm. Tumor distribution of liposomes was considerably improved by losartan pre-treatment, and target site accumulation was increased by 22%, followed by enhanced therapeutic efficacy of PTX-loaded liposomes.61

The ECM degrading strategy has also been realized by designing NPs functionalized with enzymes that degrade tumor ECM components. Hyaluronidase, degrading one of the major ECM components HA, was coupled to the surface of NPs to facilitate efficient tumor penetration. Liu and colleagues prepared a photosensitizer chlorine e6 (Ce6)-loaded NPs based on poly(maleic anhydride-alt-1-octadecene), which were modified with hyaluronidase on the surface. In vitro and in vivo studies in 4T1 tumor models showed that, comparing to NPs without surface hyaluronidase modification, the enzyme-modified NPs showed significantly improved tumor penetration and therapeutic efficacy.62 In another study, Cheng and colleagues designed PEG-PLGA NPs with surface conjugated recombinant human hyaluronidase PH 20 (rHuPH20) for improving tumor penetration. To protect the rHuPH20

and NPs in the blood circulation, they covered the rHuPH20-conjugated NPs with an extra PEG layer. The authors showed that the PEGylated NPs loaded with DOX had enhanced tumor penetration and were more effectively perfused than the physical mixture of free rHuPH20 and PLGA-PEG NPs in 4T1 mouse breast tumor model.63

In another study, collagenase was utilized to overcome the ECM barrier of tumors, which was coupled to the surface of superparamagnetic NPs. The in vivo result indicated that the collagenase-conjugated NPs were more efficiently localized in deep tumor tissues compared to non-modified NPs.64 Another report showed that the number of collagenase-modified NPs entering spheroid core in vitro was 4-fold higher than that of NPs without collagenase modification.65 Bromelain, which is one of peptidase papain family and synthesized by pineapple stems, was conjugated to silica NPs. Since bromelain as a protease can degrade tumor ECM components, the bromelain conjugation enhanced penetration of the silica NPs in matrigel by 2 times (from 500 to 1000 μm), and significantly improved NP distribution in 4T1 tumors after i.v. injection in mice was observed by intravital confocal microscopy.66

Althoug both small molecule and protein agents have been used in the ECM degrading approach, proteins are in general more difficult to be properly formulated or incorpoarted in nanomedicines. The small moelcule compound losartan, with significant ease of formulation in comparison with proteins, has been clinically used as an antihypertensive agent for decades and its safety in human has been well validated, which further demonstrates the clinical potential of losartan as a promissing agent for enhancing tumor penetration of nanomedicines.

2.4.2 Normalization of tumor vasculature—The abnormal vascular network and impaired lymphatic function of tumors lead to increased IFP that hampers tumor penetration of intravenously injected therapeutics. Therefore, normalization of tumor vasculature was hypothesized to be effective to improve the tumor penetration of drugs. As shown by Jain et al., DC101, an antibody blocking VEGFR2 signaling normalizes the morphology and function of tumor vasculature, thereby lowering the tumor IFP without affecting the lymphatic system in multiple tumor models in vivo. Consequently, the tumor penetration was increased from 7.26±1.11 to 11.23±1.41 μm by DC101 treatment, which improved the therapeutic efficacy of cytostatic drugs.67 For nanomedicines, the normalization of tumor vessel network by DC101, interestingly, only led to enhance tumor penetration of NPs of 12 nm in diameter. In contrast, penetration of larger NPs of 125 nm could not benefit from this approach, which was ascribed by the fact that DC101 decreased pore size of the walls of tumor vessels and therefore hindered the extravasation of larger NPs.68

2.4.3 Tumor vascular disruption—Vascular disrupting agents (VDA), among which combretastatin A4 phosphate (CA4P), inducing vessel disruption by inhibiting tubulin polymerization, and flavonoid acetic acid-based DMXAA, causing endothelial damage by elevated NO and serotonin production, were initially applied as cancer therapeutic agents.69 It was shown that CA4P injection increased vascular permeabilization of albumin in rats bearing P22 carcinosarcoma.70 Moreover, DMXAA pre-treatment improved extravasation of Evans Blue in C38 colon adenocarcinoma in wild type C57Bl mice, however, lower

extravasation of the dye was found in TNFα receptor-1 (TNFR1) or TNFα knockout mice, demonstrating that TNFα is essential to the penetration enhancing effect of DMXAA.71

Following the initial proof-of-concept studies, VDA, specifically CA4P, enhanced extravasation has been exploited to improve tumor penetration of nanomedicines, in which CA4P was either encapsulated in, co-injected or conjugated with nanomedicines. Folate-targeted up-conversion nanoparticles were loaded with CA4P and intravenously injected in lung adenocarcinoma ASTCa-1 inoculated mice. Local release of CA4P from the NPs inside tumor tissues induced vascular disruption by affecting the endothelial cells, which significantly enhanced tumor permeabilization in vivo.72 By co-injecting CA4P with lipid-platinum-chloride NPs in mice models, a clear vascular disruption effect was observed in UMUC3/3T3 and 4T1 tumors, and target accumulations of the NPs were increased from ~1.2 to 2.1 injected dose%/gram and from ~2.5 to 3.2 injected dose%/gram for these two tumor models, respectively.73 In a recent study, CA4P was conjugated to poly(L-glutamic acid) and the amphiphilic polymer formed NPs with CA4P in the hydrophobic core. Pharmacokinetics of the conjugated CA4P after i.v. injection was significantly improved compared to free CA4P, with an ~50-fold increase in area under the time-concentration curve, leading to a 10-fold increase in tumor accumulation of the CA4P conjugation in C26 mice than that of free CA4P 1 h post-injection. As a result, significant loss in tumor vessel density was observed 1 h after injection of both CA4P formulations, and the vascular disruption of polymer conjugated CA4P was significantly higher than of that of free CA4P 24 h post-injection.74

All the above-mentioned studies strongly support that VDA can enhance tumor vascular permeabilization and therefore tumor penetration of nanomedicines, however, systemic toxicity/side effects of VDA compromise the applicability of this strategy. To this end, physical encapsulation or chemical conjugation of VAD in drug carriers may improve the tolerability and consequently the clinical potential of these compounds.

2.5 Physical modulation of tumor microenvironment

2.5.1 Ultrasound—Ultrasound-mediated destruction of gas-filled MBs can enhance tumor penetration of NPs and antibodies via several mechanisms involving expansion and compression of MBs, micro-streams, acoustic radiation forces and high temperatures and pressures generated by destruction of MBs.53, 75 As shown in the study by Theek et al.,76 intratumoral MB destruction by ultrasound induced enhanced vessel permeabilization, which significantly improved liposome penetration in both tumor models. The amount of liposomes penetrated in deeper compartment (30-50 μm) was increased by 4% and 12% with the assistance of poly(butyl cyanoacrylate) and MicroMarker® MB under ultrasound in A431 tumor-bearing mice, respectively. In another study, the application of pulsed ultrasound in the presence of MBs resulted in increased penetration of NPs (~20 nm) by 6−20-fold in MCF-7 breast cancer spheroids, however, the penetration enhancement was attenuated with increasing particles size, i.e., NPs of 40 and 100 nm showed 9- and 3-fold of increased penetration, respectively.77 Other studies displayed that ultrasound triggered MB increased tumor penetration of polymer-coated adenovirus and monoclonal antibodies.78, 79 As one of the main clinical diagnostic modalities, ultrasound has been well utilized in the

Europe PMC Funders Author Manuscripts

clinic with high safety and ease of operation, which strengthen the clinical potential of this strategy.

2.5.2 Radiation—Radiation has also shown to enhance tumor penetration of nanomedicines, possibly by damaging tumor endothelial cells.80 Liposomal DOX was intravenously injected in mice bearing orthotopic and subcutaneous osteosarcoma. Microscopic images showed that intact liposomes were located in close proximity to endothelial cells of the tumor. However, upon radiation treatment (a single dose of 8 Gy) that did not destruct the liposomes, DOX distributed considerable further from tumor vessels, up to 450 μm in the periphery of the tumor.81 In another study, generation-8 polyamidoamine dendrimer was injected in SCCVII tumor mice model and a single radiation dose of 15 Gy significantly improved tumor penetration of the dendirmer, which was not achieved by fractionated radiation doses.82 Recently, Kunjachan et al. reported that RGD-targeted AuNPs could enhance tumor vascular disruption by radiation, in which radiation beams were restricted to the tumor with reduced radiation dose and less collateral damage to healthy tissues.83 Overall, radiation has been successfully combined with nanomedicines to achieve better tumor penetration. Apart from this effect, the intrisic therpaeutic effect of radiation can also be combined with nanomedicine treatment and therefore synergistically enhance the therapeutic efficacy.

2.5.3 Hyperthermia—Hyperthermia has been applied to enhanced penetration of nanomedicines. Hyperthermia treatment of 3D tumor models of HEYA8 and OV-90 showed significant improvement of penetration of PEG-PCL micelles.84 The hyperthermia-induced enhancement of tumor penetration of thermosensitive liposomes was also observed in xenograft models of lung carcinoma in vivo.85 Photothermal effect has shown to be able to modulate tumor tissues and enhance tumor penetration of nanomedicines. AuNRs, which absorb near infrared light and produce heat, were employed by Zhao and colleagues. They prepared AuNRs covered by mesoporous silica that was loaded with citrate-Gd and anticancer drugs (e.g. DOX). After i.v. injection, the NPs accumulated in tumor tissues by EPR effect, and comparatively deeper tumor penetration of the NPs was observed with NIR treatment of the tumor tissues, which mildly increased the local temperature to around 42-43 °C.86 Although not systemically evaluated yet, it is reasonble to expect that hyperthermia in combination with thermosensitive nanomedicines (e.g., DOX-TSL) may further increase tumor treatment efficacy due to the enhanced NP penetration and locally released small molecules with further increased tumor penetration.

2.5.4 Photochemical tissue penetration (PTP)—PTP technology that alters the epithelial barrier of tumors was realized with photosensitizers producing singlet oxygen under light illumination. Gemcitabine membrane coated drug eluting stents were combined with Ce6 to exploit PTP technology for the treatment of gastrointestinal tract obstruction by tumor growth. Due to the locally generated singlet oxygen, the epithelial layer was destroyed leading to enhanced drug penetration in tumors. The results showed that the tumor penetration was increased by 1.5-fold by PTP, and therefore improved therapeutic efficacy of the system was observed in colon tumor bearing mice.87 One potential advantage of this approach is that the therapeutic and penetration enhancing effect of singlet oxygen may

synergistically enhance the eventual treatment efficacy of nanomedicines exploiting this approach.

3 Assessment of nanomedicine penetration

The penetration capability of nanomedicines can be assessed using in vitro and in vivo models. Three types of in vitro models have been employed to study penetration of NPs, namely collagen scaffold, multicellular layers (MCLs) and tumor cell spheroids. Collagen, fibronectin and hyaluronan dominate the main composition of tumor ECM,7, 9 among which, collagen has been used as a model to mimic solid tumor matrix8 and a cell culture scaffold for tumor cells.5, 6 Another in vitro model to study the tissue penetration of NPs is MCLs. Recently, Bae et al. developed a novel in vitro model by combining MCLs and a chamber system which provided a hydraulic pressure gradient for the MCLs to simulate the IFP of tumors, with which the influence of IFP for tumor penetration of NPs could be systemically studied.88 Tumor cell spheroids are composed of malignant cells constructed within a 3D structure, and have been widely used to study penetration of nanomedicines.17, 20, 22

In vivo xenograft tumor models have been frequently used to assess tumor penetration of nanomedicines, which can be detected by ex vivo or in situ methods. For example, tumors were excised at different time points after i.v. injection of fluorescently labeled liposomes and cut into slides for fluorescence imaging examination. To obtain a whole image of tumor penetration of the liposomes, images of the individual slides were stitched together (Figure 4). The liposome distribution against depth in tumors was calculated based on the processed images.89 Kataoka and colleagues applied in vivo confocal laser scanning microscopy for the penetration assessment of drug-loaded PM in C26 and BxPC3 tumors in living mice.12 Drug-loaded PM of 30 and 70 nm were fluorescently labeled and injected in living mice, and the fluorescence intensity in tumors was detected in a real-time manner.

4 Conclusions and Future Perspectives

Several decades of nanomedicine research have resulted in a tremendous number of tumor-targeted nanochemotherapeutics. Despite the high potential, the in vivo efficacy of cancer nanomedicines, especially in clinical stages, has been suboptimal. Poor tumor penetration of nanomedicines may be one of the main reasons for their compromised therapeutic efficacy, which is caused by both the tumor pathological characteristics and improper physicochemical properties of nanomedicines. To improve tumor penetration, novel nanomedicines endowed with switchable size, penetration-promoting targeting ligands and intratumoral release have been developed. Moreover, pharmacological or physical modulations of the tumor microenvironment and vasculature have resulted in enhanced tumor penetration of nanomedicines.

Future research should be directed towards improving the clinical relevance and translational feasibility of these approaches. As reviewed above, several strategies rely on internal or external stimuli to enhance tumor penetration of nanomedicines. In this context, it should be pointed out that internal stimuli, e.g., intratumoral pH or overexpression of MMPs, can be

Europe PMC Funders Author Manuscripts

highly heterogeneous between different types of tumors. Therefore, characterization of pathological properties of tumors and/or patients is essential to be included in the development and utilization of strategies to enhance the penetration of drugs and drug delivery systems. On the other hand, externally applied physical triggers are less dependent on tumor type or pathological properties, and can then be applied in a better controlled manner in vivo. The downside of employing physical stimuli is that they are mostly active at the site of application and therefore have limited systemic effects, implying that they are not very useful for improving the treatment of metastasized tumors. Pharmacological modulators and penetration promoting agents (e.g., iRGD) can be applied via systemic administration, and therefore are suitable for both primary tumors and metastases. Future research using pharmacological modulators should take the side effects/toxicities of these agents in to account, and methods that improve the biocompatability of these compounds should be established to promote clinical translation. Overall, a variety of approaches has been developed to enhance tumor penetration of nanomedicines to achieve better therapeutic efficacy. Application of one or multiple approaches in (pre-)clinical settings has to consider the limitations and strengths of each strategy, which will eventually lead to the development of nanomedicines with robust efficacy and clinical benefit.

Acknowledgement

The authors gratefully acknowledge financial support by the German Research Foundation (DFG La2937/1-2), by the European Research Council (StG-309495-NeoNaNo and PoC-680882-CONQUEST) and by the European Union's HORIZON 2020 Programme for research, technological development and demonstration (642028 H2020-MSCA-ITN-2014).

References

(1). Lammers T, Kiessling F, Hennink WE, Storm G. J Controlled Release. 2012; 161:175–187.

(2). Couvreur P. Adv Drug Delivery Rev. 2013; 65:21–23.

(3). Wang AZ, Langer R, Farokhzad OC. Annu Rev Med. 2012; 63:185–198. [PubMed: 21888516]

(4). Zhong Y, Meng F, Deng C, Zhong Z. Biomacromolecules. 2014; 15:1955–1969. [PubMed: 24798476]

(5). Maeda H. Adv Drug Delivery Rev. 2015; 91:3–6.

(6). Deng C, Jiang Y, Cheng R, Meng F, Zhong Z. Nano Today. 2012; 7:467–480.

(7). Durymanov MO, Rosenkranz AA, Sobolev AS. Theranostics. 2015; 5:1007–1020. [PubMed: 26155316]

(8). Waite CL, Roth CM. Crit Rev Biomed Eng. 2012; 40:21–41. [PubMed: 22428797]

(9). Wilhelm S, Tavares AJ, Dai Q, Ohta S, Audet J, Dvorak HF, Chan WC. Nat Rev Mater. 2016; 1:16014–16025.

(10). Stapleton S, Milosevic M, Tannock IF, Allen C, Jaffray DA. J Controlled Release. 2015; 211:163–170.

(11). Matsumoto Y, Nichols JW, Toh K, Nomoto T, Cabral H, Miura Y, Christie RJ, Yamada N, Ogura T, Kano MR, Matsumura Y, et al. Nat Nanotechnol. 2016; 11:533–538. [PubMed: 26878143]

(12). Cabral H, Matsumoto Y, Mizuno K, Chen Q, Murakami M, Kimura M, Terada Y, Kano MR, Miyazono K, Uesaka M, Nishiyama N, et al. Nat Nanotechnol. 2011; 6:815–823. [PubMed: 22020122]

(13). Dreher MR, Liu W, Michelich CR, Dewhirst MW, Yuan F, Chilkoti A. J Natl Cancer I. 2006; 98:335–344.

(14). Popović Z, Liu W, Chauhan VP, Lee J, Wong C, Greytak AB, Insin N, Nocera DG, Fukumura D, Jain RK, Bawendi MG. Angew Chem Int Ed. 2010; 122:8831–8834.

(15). Wang J, Mao W, Lock LL, Tang J, Sui M, Sun W, Cui H, Xu D, Shen Y. ACS Nano. 2015; 9:7195–7206. [PubMed: 26149286]

(16). Vlashi E, Kelderhouse LE, Sturgis JE, Low PS. ACS Nano. 2013; 7:8573–8582. [PubMed: 24020507]

(17). Huang K, Ma H, Liu J, Huo S, Kumar A, Wei T, Zhang X, Jin S, Gan Y, Wang PC, He S, et al. ACS Nano. 2012; 6:4483–4493. [PubMed: 22540892]

(18). Campbell RB, Fukumura D, Brown EB, Mazzola LM, Izumi Y, Jain RK, Torchilin VP, Munn LL. Cancer Res. 2002; 62:6831–6836. [PubMed: 12460895]

(19). Krasnici S, Werner A, Eichhorn ME, Schmitt-Sody M, Pahernik SA, Sauer B, Schulze B, Teifel M, Michaelis U, Naujoks K, Dellian M. Int J Cancer. 2003; 105:561–567. [PubMed: 12712451]

(20). Jin S, Ma X, Ma H, Zheng K, Liu J, Hou S, Meng J, Wang PC, Wu X, Liang XJ. Nanoscale. 2013; 5:143–146. [PubMed: 23154390]

(21). Wang G, Chen Y, Wang P, Wang Y, Hong H, Li Y, Qian J, Yuan Y, Yu B, Liu C. Acta Biomater. 2016; 29:248–260. [PubMed: 26476340]

(22). Wang HX, Zuo ZQ, Du JZ, Wang YC, Sun R, Cao ZT, Ye XD, Wang JL, Leong KW, Wang J. Nano Today. 2016; 11:133–144.

(23). Torchilin VP, Klibanov AL, Huang L, O'Donnell S, Nossiff ND, Khaw BA. FASEB J. 1992; 6:2716–2719. [PubMed: 1612296]

(24). Nance E, Zhang C, Shih TY, Xu Q, Schuster BS, Hanes J. ACS Nano. 2014; 8:10655–10664. [PubMed: 25259648]

(25). Shukla S, Ablack AL, Wen AM, Lee KL, Lewis JD, Steinmetz NF. Mol Pharm. 2013; 10:33–42. [PubMed: 22731633]

(26). Chauhan VP, Popović Z, Chen O, Cui J, Fukumura D, Bawendi MG, Jain RK. Angew Chem Int Ed. 2011; 50:11417–11420.

(27). Smith BR, Kempen P, Bouley D, Xu A, Liu Z, Melosh N, Dai H, Sinclair R, Gambhir SS. Nano Lett. 2012; 12:3369–3377. [PubMed: 22650417]

(28). Black KCL, Wang Y, Luehmann HP, Cai X, Xing W, Pang B, Zhao Y, Cutler CS, Wang LV, Liu Y, Xia Y. ACS Nano. 2014; 8:4385–4394. [PubMed: 24766522]

(29). Shukla S, Eber FJ, Nagarajan AS, DiFranco NA, Schmidt N, Wen AM, Eiben S, Twyman RM, Wege C, Steinmetz NF. Adv Healthc Mater. 2015; 4:874–882. [PubMed: 25641794]

(30). Li HJ, Du JZ, Du XJ, Xu CF, Sun CY, Wang HX, Cao ZT, Yang XZ, Zhu YH, Nie S, Wang J. P Natl Acad Sci. 2016; 113:4164–4169.

(31). Li HJ, Du JZ, Liu J, Du XJ, Shen S, Zhu YH, Wang X, Ye X, Nie S, Wang J. ACS Nano. 2016; 10:6753–6761. [PubMed: 27244096]

(32). Chen Q, Feng L, Liu J, Zhu W, Dong Z, Wu Y, Liu Z. Adv Mater. 2016; 28:7129–7136. [PubMed: 27283434]

(33). Kim J, Lee YM, Kang Y, Kim WJ. ACS Nano. 2014; 8:9358–9367. [PubMed: 25184691]

(34). Ju C, Mo R, Xue J, Zhang L, Zhao Z, Xue L, Ping Q, Zhang C. Angew Chem Int Ed. 2014; 53:6253–6258.

(35). Zucker S, Vacirca J. Cancer Metast Rev. 2004; 23:101–117.

(36). Curran S, Murray GI. J Pathol. 1999; 189:300–308. [PubMed: 10547590]

(37). Wong C, Stylianopoulos T, Cui J, Martin J, Chauhan VP, Jiang W, Popović Z, Jain RK, Bawendi MG, Fukumura D. P Natl Acad Sci. 2011; 108:2426–2431.

(38). Ruan S, Cao X, Cun X, Hu G, Zhou Y, Zhang Y, Lu L, He Q, Gao H. Biomaterials. 2015; 60:100–110. [PubMed: 25988725]

(39). Hu G, Chun X, Wang Y, He Q, Gao H. Oncotarget. 2015; 6:41258–41274. [PubMed: 26517810]

(40). Tong R, Hemmati HD, Langer R, Kohane DS. J Am Chem Soc. 2012; 134:8848–8855. [PubMed: 22385538]

(41). Tong R, Chiang HH, Kohane DS. P Natl Acad Sci. 2013; 110:19048–19053.

(42). Moldenhauer D, Gröhn F. J Polym Sci Pol Phys. 2013; 51:802–816.

(43). Lee H, Fonge H, Hoang B, Reilly RM, Allen C. Mol Pharm. 2010; 7:1195–1208. [PubMed: 20476759]

(44). Peer D, Karp JM, Hong S, Farokhzad OC, Margalit R, Langer R. Nat Nanotechnol. 2007; 2:751–760. [PubMed: 18654426]

(45). Fujimori K, Covell DG, Fletcher JE, Weinstein JN. Cancer Res. 1989; 49:5656–5663. [PubMed: 2790783]

(46). Gao H, Xiong Y, Zhang S, Yang Z, Cao S, Jiang X. Mol Pharm. 2014; 11:1042–1052. [PubMed: 24521297]

(47). Sugahara KN, Teesalu T, Karmali PP, Kotamraju VR, Agemy L, Girard OM, Hanahan D, Mattrey RF, Ruoslahti E. Cancer Cell. 2009; 16:510–520. [PubMed: 19962669]

(48). Sugahara KN, Teesalu T, Karmali PP, Kotamraju VR, Agemy L, Greenwald DR, Ruoslahti E. Science. 2010; 328:1031–1035. [PubMed: 20378772]

(49). Song X, Wan Z, Chen T, Fu Y, Jiang K, Yi X, Ke H, Dong J, Yang L, Li L, Sun X, et al. Biomaterials. 2016; 108:44–56. [PubMed: 27619239]

(50). Su YL, Chen KT, Sheu YC, Sung SY, Hsu RS, Chiang CS, Hu SH. ACS Nano. 2016; 10:9420–9433.

(51). Ranney D, Antich P, Dadey E, Mason R, Kulkarni P, Singh O, Chen H, Constantanescu A, Parkey R. J Controlled Release. 2005; 109:222–235.

(52). Manzoor AA, Lindner LH, Landon CD, Park JY, Simnick AJ, Dreher MR, Das S, Hanna G, Park W, Chilkoti A, Koning GA, et al. Cancer Res. 2012; 72:5566–5575. [PubMed: 22952218]

(53). Paefgen V, Doleschel D, Kiessling F. Front Pharmacol. 2015; 6:1–16. [PubMed: 25805991]

(54). Hernot S, Klibanov AL. Adv Drug Deliver Rev. 2008; 60:1153–1166.

(55). Klibanov AL, Shevchenko TI, Raju BI, Seip R, Chin CT. J Controlled Release. 2010; 148:13–17.

(56). Geers B, Lentacker I, Sanders NN, Demeester J, Meairs S, De Smedt SC. J Controlled Release. 2011; 152:249–256.

(57). Sagnella SM, Duong H, MacMillan A, Boyer C, Whan R, McCarroll JA, Davis TP, Kavallaris M. Biomacromolecules. 2014; 15:262–275. [PubMed: 24313925]

(58). Pickup MW, Mouw JK, Weaver VM. EMBO reports. 2014:e201439246.

(59). Sakai S, Iwata C, Tanaka HY, Cabral H, Morishita Y, Miyazono K, Kano MR. J Controlled Release. 2016; 230:109–115.

(60). Diop-Frimpong B, Chauhan VP, Krane S, Boucher Y, Jain RK. P Natl Acad Sci. 2011; 108:2909–2914.

(61). Zhang L, Wang Y, Yang Y, Liu Y, Ruan S, Zhang Q, Tai X, Chen J, Xia T, Qiu Y, Gao H, et al. ACS Appl Mater Interfaces. 2015; 7:9691–9701. [PubMed: 25845545]

(62). Gong H, Chao Y, Xiang J, Han X, Song G, Feng L, Liu J, Yang G, Chen Q, Liu Z. Nano Lett. 2016; 16:2512–2521. [PubMed: 27022664]

(63). Zhou H, Fan Z, Deng J, Lemons PK, Arhontoulis DC, Bowne WB, Cheng H. Nano Lett. 2016; 16:3268–3277. [PubMed: 27057591]

(64). Kuhn SJ, Finch SK, Hallahan DE, Giorgio TD. Nano Lett. 2006; 6:306–312. [PubMed: 16464055]

(65). Goodman TT, Olive PL, Pun SH. Int J Nanomed. 2007; 2:265–274.

(66). Parodi A, Haddix SG, Taghipour N, Scaria S, Taraballi F, Cevenini A, Yazdi IK, Corbo C, Palomba R, Khaled SZ, Martinez JO, et al. ACS Nano. 2014; 8:9874–9883. [PubMed: 25119793]

(67). Tong RT, Boucher Y, Kozin SV, Winkler F, Hicklin DJ, Jain RK. Cancer Res. 2004; 64:3731–3736. [PubMed: 15172975]

(68). Chauhan VP, Stylianopoulos T, Martin JD, Popović Z, Chen O, Kamoun WS, Bawendi MG, Fukumura D, Jain RK. Nat Nanotechnol. 2012; 7:383–388. [PubMed: 22484912]

(69). Tozer GM, Kanthou C, Baguley BC. Nat Rev Cancer. 2005; 5:423–435. [PubMed: 15928673]

(70). Tozer GM, Prise VE, Wilson J, Cemazar M, Shan S, Dewhirst MW, Barber PR, Vojnovic B, Chaplin DJ. Cancer Res. 2001; 61:6413–6422. [PubMed: 11522635]

(71). Zhao L, Ching LM, Kestell P, Kelland LR, Baguley BC. Int J Cancer. 2005; 116:322–326. [PubMed: 15800918]

(72). Wei Y, Chen Q, Wu B, Zhou A, Xing D. Nanoscale. 2012; 4:3901–3909. [PubMed: 22652931]

(73). Satterlee AB, Rojas JD, Dayton PA, Huang L. Theranostics. 2017; 7:253–269. [PubMed: 28042332]

(74). Liu T, Zhang D, Song W, Tang Z, Zhu J, Ma Z, Wang X, Chen X, Tong T. Acta Biomater. 2017 In press.

(75). Dasgupta A, Liu M, Ojha T, Storm G, Kiessling F, Lammers T. Drug Discov Today Tech. 2016; 20:41–48.

(76). Theek B, Baues M, Ojha T, Möckel D, Veettil SK, Steitz J, van Bloois L, Storm G, Kiessling F, Lammers T. J Controlled Release. 2016; 231:77–85.

(77). Grainger SJ, Serna JV, Sunny S, Zhou Y, Deng CX, El-Sayed MEH. Mol pharm. 2010; 7:2006–2019. [PubMed: 20957996]

(78). Carlisle R, Choi J, Bazan-Peregrino M, Laga R, Subr V, Kostka L, Ulbrich K, Coussios CC, Seymour LW. J Natl Cancer I. 2013; 105:1701–1710.

(79). Wang S, Shin IS, Hancock H, Jang BS, Kim HS, Lee SM, Zderic V, Frenkel V, Pastan I, Paik CH, Dreher MR. J Controlled Release. 2012; 162:218–224.

(80). Potchen EJ, Kinzie J, Curtis C, Siegel BA, Studer RK. Cancer. 1972; 30:639–642. [PubMed: 4677852]

(81). Davies, CdL, Lundstrøm, LM., Frengen, J., Eikenes, L., Bruland, ØS., Kaalhus, O., Hjelstuen, MHB., Brekken, C. Cancer Res. 2004; 64:547–553. [PubMed: 14744768]

(82). Kobayashi H, Reijnders K, English S, Yordanov AT, Milenic DE, Sowers AL, Citrin D, Krishna MC, Waldmann TA, Mitchell JB, Brechbiel MW. Clin Cancer Res. 2004; 10:7712–7720. [PubMed: 15570005]

(83). Kunjachan S, Detappe A, Kumar R, Ireland T, Cameron L, Biancur DE, Motto-Ros V, Sancey L, Sridhar S, Makrigiorgos GM, Berbeco RI. Nano Lett. 2015; 15:7488–7496. [PubMed: 26418302]

(84). Eetezadi S, De Souza R, Vythilingam M, Cataldi RL, Allen C. Mol Pharm. 2015; 12:3973–3985. [PubMed: 26394060]

(85). Dou YN, Dunne M, Huang H, Mckee T, Chang MC, Jaffray DA, Allen C. J Drug Target. 2016; 24:865–877. [PubMed: 27310112]

(86). Wang J, Liu J, Liu Y, Wang L, Cao M, Ji Y, Wu X, Xu Y, Bai B, Miao Q, Chen C, Zhao Y. Adv Mater. 2016; 28:8950–8958. [PubMed: 27562240]

(87). Min D, Jeong D, Choi MG, Na K. Biomaterials. 2015; 52:484–493. [PubMed: 25818454]

(88). Suzuki H, Bae YH. Biomaterials. 2016; 98:120–130. [PubMed: 27182814]

(89). Ekdawi SN, Stewart JM, Dunne M, Stapleton S, Mitsakakis N, Dou YN, Jaffray DA, Allen C. J Controlled Release. 2015; 207:101–111.

Europe PMC Funders Author Manuscripts

Europe PMC Funders Author Manuscripts

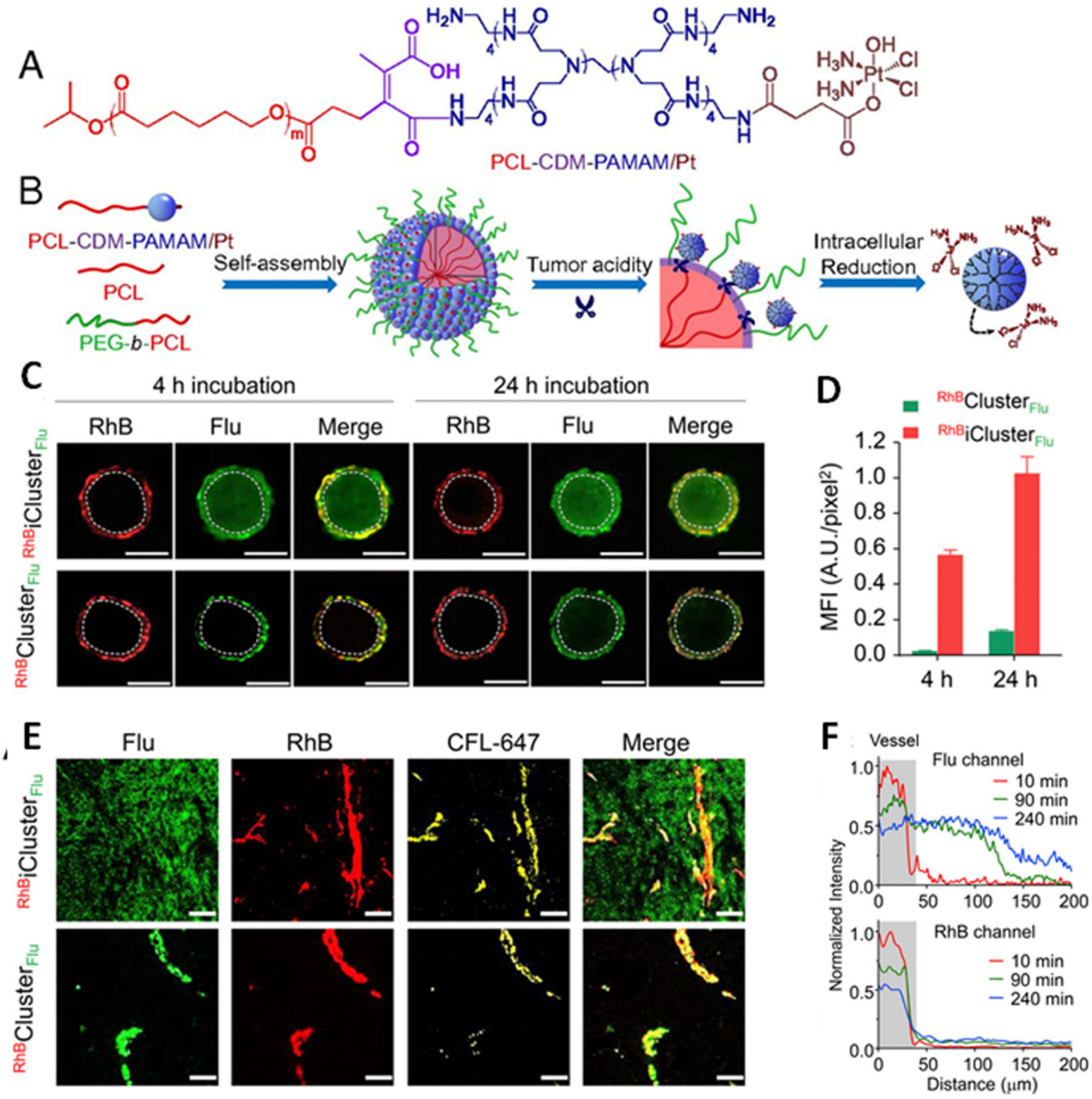

Figure 1.

(A) Chemical structure of PCL-CDM-PAMAM/Pt. (B) Self-assembly and structural change of iCluster in response to tumor acidity. The platinum prodrug-conjugated poly(amidoamine) (PAMAM/Pt) was conjugated to PCL via a pH sensitive linker which was cleaved in the tumor acidic environment, leading to release of the prodrug that showed enhanced tumor penetration due to its smaller size and thereafter intracellular release of Pt. (C) In vitro penetration of $^{RhB}iCluster_{Flu}$ and $^{RhB}Cluster_{Flu}$ in cellular spheroids at pH 6.8 after 4- or 24-h of incubation. $^{RhB}iCluster_{Flu}$ and $^{RhB}Cluster_{Flu}$ were labeled with

fluorescein (Flu, green) on PAMAM and with rhodamine B (RhB, red) on the PCL component. The circles were considered inside area of the spheroids. (Scale bar, 200 μm.) (D) Mean fluorescence intensity (MFI) of green signals (representing PAMAM) in the cellular spheroids. Significantly higher distribution of iCluster inside the spheroids was presented 4-h post-injection compared to that of Cluster. (E) In vivo tumor distribution of $^{RhB}iCluster_{Flu}$ and $^{RhB}Cluster_{Flu}$ 4-h post-injection. Flu (green): PAMAM, RhB (red): PCL core and yellow: blood vessels. (Scale bar, 50 μm.) Extravasation of PAMAM in $^{RhB}iCluster_{Flu}$ from tumor vessels to tumor interstitia was observed whereas that of $^{RhB}Cluster_{Flu}$ was negligible. (F) Tumor distribution of PAMAM from $^{RhB}iCluster_{Flu}$. Time-dependent increase of Flu signal (PAMAM) is shown in the upper panel, demonstrating enhanced penetration of PAMAM, and no significant change of the RhB signal was observed (lower panel) pointing to that there was insignificant penetration of the PCL core. Reprinted from reference [30]. Copyright [2016]. United States National Academy of Sciences.

Europe PMC Funders Author Manuscripts

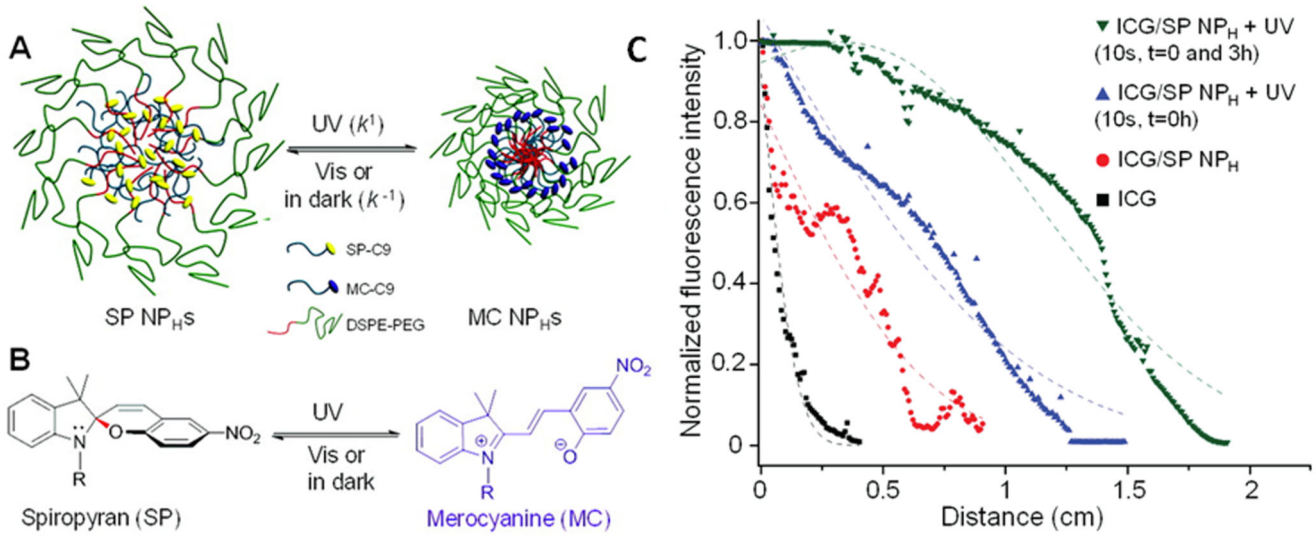

Figure 2.

(A) Schematic representation of photoswitching NPs (SP NP$_H$s) composed of SP-C9 and DSPE-PEG. (B) Structure and photoisomerization reaction between spiropyran (SP) and merocyanine (MC). Under UV illumination, the hydrophobic SP-C9 was converted to amphiphilic merocyanine (MC)-C9 and the size of the SP-C9 NPs was decreased due to the solubility change of SP-C9, which led to better penetration of the NPs because of their decreased size. (C) Penetration distances of ICG-loaded SP NPs in collagen gel matrix under UV irradiation 12-h post-incubation. The penetration distance of SP NPs was significantly increased by 10 s of UV irradiation applied immediately after incubation (blue curve), and an additional UV irradiation further enhanced the penetration distance (green curve). Reprinted from reference [40]. Copyright [2012]. American Chemical Society.

Europe PMC Funders Author Manuscripts

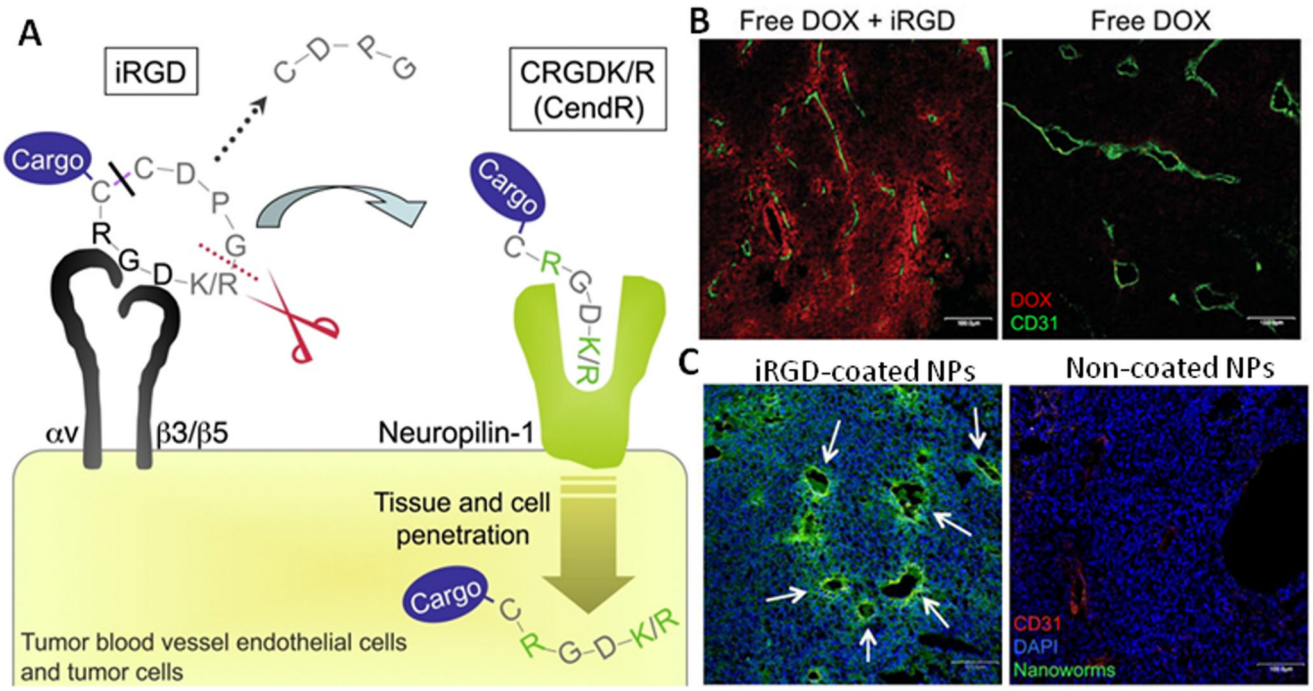

Figure 3.

Multistep Binding and Penetration Mechanism of iRGD and enhancement of tumor penetration of free DOX and NPs by co-injected or conjugated iRGD. (A) Mechanism of iRGD enhanced tumor penetration. The RGD motif of iRGD mediates binding to αv integrins on the surface of tumor endothelium, and thereafter a proteolytic cleavage exposes a binding motif for neuropilin-1, which mediates penetration into tissues and cells. (B) Tumor penetration of free DOX co-administered with iRGD was significantly improved (left panel) compared to that without co-injection of iRGD (right panel). Red: DOX; green: vessels. (C) iRGD-coated NPs extravasated into tumor interstitium (left panel), which was not achieved with non-coated NPs (right panel). Green: iRGD-coated NPs; red: vessels; blue: DAPI. Reprinted from reference [47 and 48]. Copyright [2009 and 2010]. Cell Press and American Association for the Advancement of Science (United States).

Europe PMC Funders Author Manuscripts

Europe PMC Funders Author Manuscripts

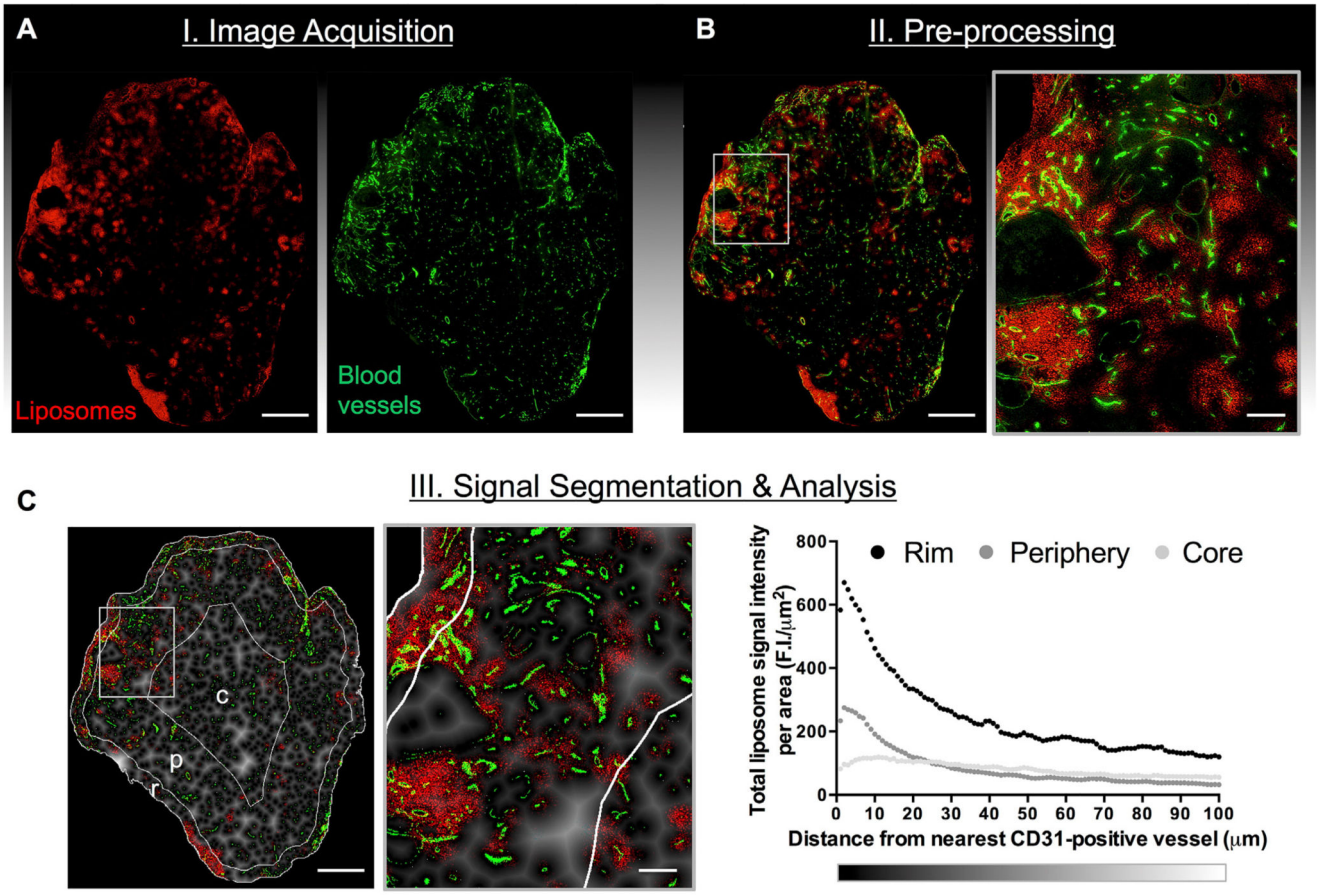

Figure 4.

Representation of fluorescence image analysis process. A-B: Separate images of liposome (red) and blood vessel (BV, green), and aligned as shown in panel B. C: The singles of liposomes and blood vessels were quantified using a customized MATLAB algorithm, and the distance of liposomes migrated from the selected vessel was calculated (right panel). Reprinted from reference [89]. Copyright [2015]. Elsevier.